

This discussion paper is/has been under review for the journal Ocean Science (OS).
Please refer to the corresponding final paper in OS if available.

Increasing transports of volume, heat, and salt towards the Arctic in the Faroe Current 1993–2013

B. Hansen¹, K. M. H. Larsen¹, H. Hátún¹, R. Kristiansen¹, E. Mortensen¹, and
S. Østerhus²

¹Faroe Marine Research Institute, Tórshavn, Faroe Islands

²Uni Research Climate, Bergen, Norway

Received: 24 April 2015 – Accepted: 17 May 2015 – Published: 9 June 2015

Correspondence to: B. Hansen (bogihan@hav.fo)

Published by Copernicus Publications on behalf of the European Geosciences Union.

OSD

12, 1013–1050, 2015

Increasing transports
of volume, heat, and
salt towards the
Arctic in the Faroe
Current 1993–2013

B. Hansen et al.

Title Page

Abstract

Introduction

Conclusions

References

Tables

Figures

◀

▶

Back

Close

Full Screen / Esc

Printer-friendly Version

Interactive Discussion



Abstract

The flow of warm and saline water from the Atlantic Ocean, across the Greenland–Scotland Ridge, into the Nordic Seas – the Atlantic inflow – is split into three separate branches. The most intensive of these branches is the inflow between Iceland and the Faroe Islands (Faroes), which is focused into the Faroe Current, north of the Faroes. The Atlantic inflow is an integral part of the North Atlantic thermohaline circulation (THC), which is projected to weaken during the 21 century and might conceivably reduce the oceanic heat and salt transports towards the Arctic. Since the mid-1990s, hydrographic properties and current velocities of the Faroe Current have been monitored along a section extending north from the Faroe shelf. From these in situ observations, time series of volume, heat, and salt transport have previously been reported, but the high variability of the transport series has made it difficult to identify trends. Here, we present results from a new analysis of the Faroe Current where the in situ observations have been combined with satellite altimetry. For the period 1993 to 2013, we find the average volume transport of Atlantic water in the Faroe Current to be 3.8 ± 0.5 Sv ($1\text{ Sv} = 10^6 \text{ m}^3 \text{ s}^{-1}$) with a heat transport relative to 0°C of 124 ± 15 TW ($1\text{ TW} = 10^{12} \text{ W}$). Consistent with other results for the Northeast Atlantic component of the THC, we find no indication of weakening. The transports of the Faroe Current, on the contrary, increased. The overall trend over the two decades of observation was $9 \pm 8\%$ for volume transport and $18 \pm 9\%$ for heat transport (95 % confidence intervals). During the same period, the salt transport relative to the salinity of the deep Faroe Bank Channel overflow (34.93) more than doubled, potentially strengthening the feedback on thermohaline intensity. The increased heat and salt transports are partly caused by the increased volume transport and partly by increased temperatures and salinities of the Atlantic inflow, attributed mainly to the weakened subpolar gyre.

OSD

12, 1013–1050, 2015

Increasing transports of volume, heat, and salt towards the Arctic in the Faroe Current 1993–2013

B. Hansen et al.

	Title Page
Abstract	Introduction
Conclusions	References
Tables	Figures
◀	▶
◀	▶
Back	Close
Full Screen / Esc	
Printer-friendly Version	
Interactive Discussion	

1 Introduction

The flow of warm and saline water from the Atlantic Ocean, across the Greenland–Scotland Ridge, into the Nordic Seas, the *Atlantic inflow*, occurs in three separate branches (plus flow over continental shelf areas). The two main branches pass between Iceland and the Scottish shelf on either side of the Faroes (Faroe Islands). This study treats the branch that flows between Iceland and the Faroes, the *IF-inflow* (Fig. 1a), across the Iceland–Faroe Ridge (IFR) and continues in the *Faroe Current*.

This flow carries heat towards the Arctic and is an integral part of the North Atlantic thermohaline circulation (THC), which is projected to weaken due to global warming (Collins et al., 2013). It has therefore long been an ambition to monitor its transport of water (volume, mass), heat, and salt. The hydrographic properties (temperature and salinity) of the Faroe Current have been monitored along a section, *section N*, extending northwards from the Faroes since the late 1980s. In the mid-1990s, this section was instrumented with moored Acoustic Doppler Current profilers (ADCPs) to monitor the transports (Fig. 1b). During and after crossing the IFR, the Atlantic water meets colder and less saline water masses, which here are collectively termed *Arctic water*. In this study, we focus on the Atlantic water component of the Faroe Current as it passes through section N.

A priori, it might seem inappropriate to locate the monitoring section downstream of the IFR rather than on it, but the ridge is wide and inflow has been reported to occur over most of its width (Orvik and Niiler, 2002; Jakobsen et al., 2003; Rossby et al., 2009). Strong mesoscale activity and the counterflow of cold overflow water (IF-overflow) below the Atlantic water also requires high spatial resolution of velocity as well as temperature and salinity measurements. Monitoring on the IFR would therefore require a prohibitively large number of moorings, which would have to be protected from fishing gear. The chosen monitoring section, section N, in contrast, has a much more focused inflow, where most of the ADCPs may be deployed sufficiently deep to

OSD

12, 1013–1050, 2015

Increasing transports
of volume, heat, and
salt towards the
Arctic in the Faroe
Current 1993–2013

B. Hansen et al.

Title Page	
Abstract	Introduction
Conclusions	References
Tables	Figures
◀	▶
◀	▶
Back	Close
Full Screen / Esc	
Printer-friendly Version	
Interactive Discussion	

**Increasing transports
of volume, heat, and
salt towards the
Arctic in the Faroe
Current 1993–2013**

B. Hansen et al.

[Title Page](#)[Abstract](#)[Introduction](#)[Conclusions](#)[References](#)[Tables](#)[Figures](#)[|◀](#)[▶|](#)[◀](#)[▶](#)[Back](#)[Close](#)[Full Screen / Esc](#)[Printer-friendly Version](#)[Interactive Discussion](#)

avoid loss from fishing gear. Only over the relatively narrow Faroe slope is it necessary to protect the ADCPs by bottom mounted frames (sites NA and NE on Fig. 1b).

After some initial experimentation, an ADCP array with three moorings (NA, NB, and NC) started monitoring in summer 1997. The array has been altered and mooring sites have been changed, but as a whole, it has continued operating since then, although with gaps during annual servicing and due to instrument failure or loss. In parallel, regular CTD (Conductivity, Temperature, Depth) cruises have gathered hydrographic data at standard stations (Fig. 1), usually 3–5 times a year.

Based on the combined CTD and ADCP data sets, time series of volume transport and heat and salt transport were reported in 2003 (Hansen et al., 2003) for the 1997–2000 period and in 2010 (Hansen et al., 2010) for the 1997–2008 period. In both cases, the transport values were based on the in situ data (CTD and ADCP), solely, using the methodology described in Hansen et al. (2003). It appeared that there was good correspondence between these in situ based estimates and satellite altimetry (Hátún and Mc Climans, 2003; Hansen et al., 2010) and it was recognized that better estimates might be made by combining the in situ observations with satellite altimetry.

We have therefore re-analyzed the complete updated data set including both the in situ data and altimetry data from a line of grid points parallel to and close to the monitoring section (Fig. 1b). This task involves a large number of technical issues that will not be detailed here. These details are described in a technical report (Hansen et al., 2015), which we will refer to repeatedly. The report is available on: www.hav.fo/PDF/Ritgerdir/2015/TecRep1501.pdf.

In this paper, we focus on the main results from the analysis, which are the time series of volume, heat and salt transport by the Atlantic water component of the Faroe Current. We report average values and estimate seasonal variations, but the main aim is to resolve, whether any of the transport series exhibit long-term trends, and to quantify them.

2 Material and methods

All the in situ observations (available at www.envofar.fo) are collected along section N (Fig. 1). Altimetry data are selected along a line following longitude 6.125° W, which is so close that we consider it to be along the same section.

5 2.1 Hydrographic observations

Fourteen standard stations, labeled N01 to N14, are located equidistantly along section N following 6.083° W with a separation of 10 nautical miles from N01 at 62.333° N to N14 at 64.5° N (N14 is at longitude 6.000° W). Typically, the section has been occupied on 4 cruises each year since 1988 although bad weather and other conditions
10 have prevented complete coverage in some cases. Thus, some stations have been occupied almost a hundred times, but others considerably less often, especially in the northernmost part.

We use quality controlled and calibrated CTD data averaged to meter intervals with a main focus on data between stations N02 and N11, which contain that part of the section through which the Atlantic water passes. Accuracy is better than 0.01 °C for temperature and 0.01 for salinity throughout the period although salinity spikes in strong thermoclines may exceed this threshold prior to 1997 when the high quality (SeaBird 911+) CTD model was first acquired.
15

2.2 In situ current velocity observations

20 Between January 1996 and May 2014, ADCPs have been moored at seven different sites along the section (Table 1). Each site is labelled by a two-letter code beginning with “N”. At two sites (NF and ND), only single deployments were made. The other sites have had repeated deployments, with moorings usually deployed in summer one year and recovered the year after. Thus, there are typically gaps of 2–4 weeks every
25 summer.

OSD

12, 1013–1050, 2015

Increasing transports
of volume, heat, and
salt towards the
Arctic in the Faroe
Current 1993–2013

B. Hansen et al.

Title Page	
Abstract	Introduction
Conclusions	References
Tables	Figures
◀	▶
◀	▶
Back	Close
Full Screen / Esc	
Printer-friendly Version	
Interactive Discussion	

The most complete coverage has been when all four “long-term” sites (NA + NE + NB + NG) were occupied, from summer 2000 to summer 2001 and from summer 2004 to summer 2011. At most sites, the ADCPs have been deployed in the top of traditional moorings at sufficient depth to prevent loss from fishing gear. At the shallow sites, NA and NE, it has been necessary to put the ADCPs into protective buoyant frames attached by acoustic releases to concrete anchors deployed on the bottom (Hansen et al., 2015, Fig. 2.2.1). The ADCPs have typically pinged every 20 min (single pings). After extensive editing and quality control, the data have been averaged to daily values with accuracy $\approx 0.2 \text{ cm s}^{-1}$ and extrapolated to the surface (Hansen et al., 2015, Fig. 2.2.2). We also use the bottom temperature measured by the ADCP temperature sensor at site NE, T_{NE} , close to the typical boundary between Atlantic and Arctic water masses (Fig. 1b). This sensor may have offsets several tenths of a degree, but that is adequate for our purpose.

2.3 Satellite altimetry

Daily averaged altimetry was selected from the global gridded ($0.25^\circ \times 0.25^\circ$) sea level anomaly (SLA) field available from “<http://www.aviso.altimetry.fr>”. SLA values were selected for 8 grid points, which we label A_1 to A_8 , along 6.125°W from 62.125°N to 63.875°N (Fig. 1b). For each of these points, we have sea level anomalies $H_k(t)$, $k = 1$ to 8, for 7791 days from 1 January 1993 to 1 May 2014. An Empirical Orthogonal Function (EOF) analysis revealed that the first two modes explained 95 % of the variance with 87 % in the first mode (Hansen et al., 2015, Fig. 2.4.1). The associated principal components (temporal variation) are denoted $\text{PC}_1(t)$ and $\text{PC}_2(t)$, respectively (Hansen et al., 2015, Fig. 2.4.2). The EOF modes also revealed that the flow variations are confined to the region north of A_2 , which is the region we will focus on.

At time scales exceeding a few days, we expect approximate geostrophic balance, so that the horizontally averaged eastward surface ($z = 0$) velocity $U_k(0, t)$ between grid points A_k and A_{k+1} is proportional to the difference in absolute sea level height (SLH) between the two points. The SLA values do not represent absolute SLH (above

[Title Page](#)[Abstract](#)[Introduction](#)[Conclusions](#)[References](#)[Tables](#)[Figures](#)[|◀](#)[▶|](#)[◀](#)[▶](#)[Back](#)[Close](#)[Full Screen / Esc](#)[Printer-friendly Version](#)[Interactive Discussion](#)

the geoid), but rather the anomaly. Surface velocities derived from SLA differences between two grid points are therefore also anomalies, but may be made absolute by adding a constant U_k^0 for each interval:

$$U_k(0, t) = \frac{g}{f \cdot L} \cdot [H_k(t) - H_{k+1}(t)] + U_k^0 \quad (1)$$

- 5 where g and f are gravity and Coriolis parameter, respectively, and L is the distance between the altimetry grid points. The constants U_k^0 for each altimetry interval are determined from ADCP data and average geostrophic profiles that are derived from the CTD data (Hansen et al., 2015, Table 2.4.4).

2.4 Combining ADCP and altimetry to generate velocity at depth

- 10 Once calibrated by Eq. (1), the altimetry data provide us with a time series of horizontally averaged eastward surface velocity $U_k(0, t)$ for each altimetry interval A_k to A_{k+1} . To find the horizontally averaged velocity $U_k(z, t)$ for interval k at depth z , we multiply the surface velocity $U_k(0, t)$ by a function $\phi_k(z, t)$, which we term the *relative profile*:

$$U_k(z, t) = U_k(0, t) \cdot \phi_k(z, t) \quad (2)$$

- 15 In periods with good ADCP coverage in an interval A_k to A_{k+1} , the temporally varying relative profile $\phi_k(z, t)$ may be determined for each day from the ADCP data (Hansen et al., 2015, Eq. 5.1.2), but much of the time, we have to replace $\phi_k(z, t)$ by an average relative profile $\Phi_k(z)$ for each interval. The average relative profiles are based on average ADCP profiles and on average geostrophic profiles, calculated from the CTD data (Hansen et al., 2015, Fig. 3.2.2).

2.5 Calculation of transport time series

With the eastward surface velocity $U_k(0, t)$ determined from calibrated altimetry by Eq. (1) and its vertical variation $U_k(z, t)$ given by Eq. (2), time series of volume trans-

port, $Q(t)$, between grid points A_2 and A_8 , may be determined as:

$$Q(t) = \sum_{k=2}^7 \sum_{z=1}^{600} U_k(z, t) \cdot W_k(z, t) \quad (3)$$

where $W_k(z, t)$ is the width of the interval from A_k to A_{k+1} at depth z and time t . If we want to integrate down to 600 m all along the section, then $W_k(z, t) = L$, the distance between grid points, for all k , z , and t , except where the bottom is shallower than 600 m. More generally, we may wish to integrate down to a certain boundary (e.g., the 4 °C isotherm) that varies in depth along the section and also with time. In that case, we can write $W_k(z, t) = L \cdot r_k(z, t)$ where $r_k(z, t)$ is the fraction (between 0 and 1) of the width of altimetry interval k at depth z that is above the boundary or bottom at time t .

To calculate heat transport relative to a specified reference temperature T_{Ref} , we use:

$$Q_{\text{Heat}}(t) = \rho \cdot C_H \cdot \sum_{k=2}^7 \sum_{z=1}^{600} [T_k(z, t) - T_{\text{Ref}}] \cdot U_k(z, t) \cdot W_k(z, t) \quad (4)$$

where ρ is density, C_H is the specific heat, and $T_k(z, t)$ is the temperature at depth z and time t , horizontally averaged from A_k to A_{k+1} .

The salt transport through section N by Atlantic water is well defined in an absolute sense. Every cubic metre passing across the IFR with a salinity S given in practical salinity units represents an input of salt to the Nordic Seas (Fig. 1a) equal to $\rho \cdot C_S \cdot S \text{ kg}$ where C_S is an (approximately constant) factor converting from practical to absolute salinity. The salt transport, relative to some specified reference salinity S_{Ref} , is therefore given by:

$$Q_{\text{Salt}}(t) = \rho \cdot C_S \cdot \sum_{k=2}^7 \sum_{z=1}^{600} [S_k(z, t) - S_{\text{Ref}}] \cdot U_k(z, t) \cdot W_k(z, t) \quad (5)$$

Title Page	
Abstract	Introduction
Conclusions	References
Tables	Figures
◀	▶
◀	▶
Back	Close
Full Screen / Esc	
Printer-friendly Version	
Interactive Discussion	

3 Results

The basic results of this study are the characteristics of the velocity field, generated by combining ADCP and altimetry data, and the characteristics of the temperature and salinity fields, mainly based on the CTD observations. By combining these results, we can produce continuous time series of Atlantic water characteristics (T and S) and spatial extent on the section and we can simulate distributions of velocity, temperature, and salinity with reasonable accuracy. Together, these series allow us to generate the main results: continuous time series of volume, heat, and salt transport for the whole altimetry period.

10 3.1 Velocity distribution on the section

The average velocity profiles from the ADCPs and from geostrophy (Fig. 2) are compatible. We also find that the relative profiles – the $\varphi_k(z, t)$ functions defined in Sect. 2.4 – are consistent in shape. This is verified by correlating the extrapolated eastward surface velocity and the vertically averaged eastward velocity for individual long-term 15 ADCP sites. For weekly averages, we find correlation coefficients between 0.94 and 0.98 (Hansen et al., 2015, Table 3.2.1 and Fig. 3.2.1). This indicates that replacing $\varphi_k(z, t)$ by the average relative profile $\Phi_k(z)$ in Eq. (2) should generally be a good approximation.

After extrapolation to the surface, average eastward velocities for the four long-term 20 ADCP sites (Table 1) were used to calibrate the altimetric surface velocities between A_3 and A_5 (Hansen et al., 2015, Table 2.4.1), i.e., to determine the offset values U_3^0 and U_4^0 in Eq. (1). Values for U_k^0 in the other altimetry intervals (red lines in Fig. 3) were determined from average geostrophic profiles combined with deep current measurements (Hansen et al., 2015, Table 2.4.3).

OSD

12, 1013–1050, 2015

Increasing transports
of volume, heat, and
salt towards the
Arctic in the Faroe
Current 1993–2013

B. Hansen et al.

Title Page	
Abstract	Introduction
Conclusions	References
Tables	Figures
◀	▶
◀	▶
Back	Close
Full Screen / Esc	
Printer-friendly Version	
Interactive Discussion	

3.2 Temperature and salinity distributions

In the CTD data set, there are 78 cruises with complete coverage from station N02 to N11 in the period 1993 to 2013. The average temperature (Fig. 4a) and salinity (Fig. 4c) distributions on the section illustrate the characteristic difference between the warm and saline Atlantic water and the colder and less saline Arctic water masses except that seasonal heating blurs the water mass characteristics in the uppermost layers in the northern part of the section (Hansen et al., 2015, Fig. 4.1).

Seasonal heating is also indicated by a relatively high standard deviation of temperature in the near-surface layer, but the highest standard deviations for both temperature and salinity are in the pycnocline region (Fig. 4b and d) and illustrate variations in Atlantic water extent.

To a large extent, the variations in hydrographic properties may be seen as composed of three different contributions: (1) long-term variations in the temperature and salinity of the Atlantic water, (2) seasonal variations, especially of temperature near the surface, and (3) variations in the extent of the Atlantic water on the section downwards and northwards (frontal variations).

3.2.1 Atlantic water temperature and salinity

As seen in Fig. 4, the southernmost stations over the shelf and inner slope are usually dominated by Atlantic water (reddish colours) and this region has also been most frequently sampled in the CTD cruises. We have therefore generated a time series of Atlantic water temperature by averaging temperature between 100 and 150 m depth at station N03. This time series is termed $T_A(t)$. For the Atlantic water salinity, we use the previously reported “Atlantic core salinity”, $S_A(t)$, which represents the most saline water on the section during each individual cruise (Larsen et al., 2012).

For both of these parameters, we have extracted the seasonal (Hansen et al., 2015, Figs. 4.5.3 and 4.7.1) and the long-term variations (Fig. 5) using an iterative procedure (Hansen et al., 2015, Appendix B). The Atlantic water temperature increased about 1 °C

OSD

12, 1013–1050, 2015

Increasing transports
of volume, heat, and
salt towards the
Arctic in the Faroe
Current 1993–2013

B. Hansen et al.

Title Page

Abstract

Introduction

Conclusions

References

Tables

Figures

◀

▶

◀

▶

Back

Close

Full Screen / Esc

Printer-friendly Version

Interactive Discussion



from 1993 to 2003, after which there are no consistent trends. The salinity changes of the Atlantic core parallel the temperature changes with an overall increase of about 0.1.

3.2.2 Simulating daily values for Atlantic water extent on the section

- 5 The seasonal variations of temperature and salinity at all points on the section may be estimated by fitting a sinusoidal seasonal signal to the CTD data, and they are most pronounced in the uppermost 100 m layer (Hansen et al., 2015, Fig. 4.6.1). At greater depth, the variations are dominated by the movement of the thermo- and halocline. To describe this, we choose the 4 °C isotherm, which is roughly intermediate between the 10 temperatures of the Atlantic and the deep Arctic waters. The depth of this isotherm at station j and time t is denoted $D_j(t)$.

From direct observations, we only know the depth of this isoline at the times of CTD cruises. As shown by Hátún et al. (2004), the temperature (and salinity) field is, however, linked to the velocity field, which again is linked to the altimetry. To investigate 15 this, all CTD cruises since 1993 were analyzed to find the depth of the 4 °C isotherm at stations N04 to N11. No clear long-term trend or seasonal variation were evident (Hansen et al., 2015, Fig. 4.2.1). These depth values were then correlated with various parameters that might be considered to influence isotherm depth (Hansen et al., 2015, Table 4.2.1).

20 For most stations, the altimetry data provided the best indicator of the 4 °C isotherm depth and a multiple linear regression on two separate altimetry parameters could explain between 56 and 65 % of the variance in 4 °C isotherm depth for the five stations from N05 to N09. For stations N10 and N11, the explained variance decreased to 47 and 42 %, respectively (Hansen et al., 2015, Table 4.2.1).

25 For station N04, only 30 % of the 4 °C isotherm variance could be explained by altimetry and ADCP velocity data, solely, but the inclusion of bottom temperature observed at ADCP site NE increased the explained variance to 58 %. This site is located where the thermocline typically intersects the bottom (Fig. 1b) and the bottom temperature

[Title Page](#)

[Abstract](#)

[Introduction](#)

[Conclusions](#)

[References](#)

[Tables](#)

[Figures](#)

[◀](#)

[▶](#)

[◀](#)

[▶](#)

[Back](#)

[Close](#)

[Full Screen / Esc](#)

[Printer-friendly Version](#)

[Interactive Discussion](#)



Title Page	
Abstract	Introduction
Conclusions	References
Tables	Figures
◀	▶
◀	▶
Back	Close
Full Screen / Esc	
Printer-friendly Version	
Interactive Discussion	

exhibits large variations – even on monthly timescales (Hansen et al., 2015, Fig. 4.3.1) – that indicate Atlantic water extent in the area.

Using the coefficients from these regression analyses, the depth of the 4 °C isotherm at most stations may be simulated with reasonable accuracy for every day with altimetry data, i.e., since 1 January 1993. Especially for days in this period with bottom temperature measurement at site NE, we can simulate the 4 °C isotherm depth from its intersect with the Faroe slope north to station N09, explaining more than half of its total variance.

At station N09, the isotherm already approaches the surface and has diverged from the 35.0 isohaline (Fig. 1b). Here, temperature is no longer a good indicator of Atlantic water extent. To simulate the northern boundary of the Atlantic water extent, we instead seek to simulate the location of the 35.0 isohaline in the near-surface layer (Fig. 1b). This was also explored by multiple linear regressions on various altimetry parameters using CTD observations from the 1997 to 2013 period, for which the salinity data have the best quality. Based on this, an algorithm was developed that allowed simulation of the latitude of the 35.0 isohaline at 100 m depth from altimetry data, explaining 44 % of its variance (Hansen et al., 2015, Fig. 4.4.1), and defining the northern boundary of the Atlantic water extent for the top 100 m layer.

3.2.3 Simulating daily temperature and salinity fields

With continuous simulation of the boundary of Atlantic water extent, Eqs. (1) to (3) allow calculation of the volume transport of Atlantic water, but for heat and salt transport, we need continuous simulations of temperature and salinity distributions on the section, as well. To develop these, we used the CTD data from all the 78 cruises 1993 to 2013 that had complete coverage from station N02 to N11. We found that the temperature distribution is well explained as a linear combination of a seasonal signal, the Atlantic water temperature, $T_A(t)$ (Fig. 5) and the depth of the 4 °C isotherm $D_j(t)$. For stations

N04 to N11, the temperature $T_j(z, t)$ at station j , depth z , and time t is expressed as:

$$T_j(z, t) = T_j^{\text{Seas}}(z, t) + a_j(z) \cdot T_A(t) + b_j(z) \cdot D_j(t) + c_j(z) \quad (6)$$

In this expression, $T_j^{\text{Seas}}(z, t)$ is a sinusoidal seasonal variation determined by regression (Hansen et al., 2015, Fig. 4.6.1). The regression coefficients a , b , and c depend on the station number (latitude) and depth, but not on time. For stations N02 and N03, where the 4 °C isotherm would have been below the bottom, we use the principal component $\text{PC}_1(t)$ from the altimetry instead of $D_j(t)$ in Eq. (6). The explanatory power of this expression varies across the section, but over the average Atlantic water extent, Eq. (6) explains 61 % of the total variance, on average (Hansen et al., 2015, Fig. 4.6.2).

For salinity, the seasonal variation is less pronounced (Hansen et al., 2015, Fig. 4.8.1). To simulate the salinity at station j ($j = 4$ to 11), depth z , and time t , $S_j(z, t)$, we therefore use the expression:

$$S_j(z, t) = d_j(z) \cdot S_A(t) + e_j(z) \cdot D_j(t) + f_j(z) \quad (7)$$

where $S_A(t)$ is the salinity of the Atlantic water (Fig. 5) and d , e , and f are regression coefficients. At stations N02 and N03, $D_j(t)$ is again replaced by $\text{PC}_1(t)$. On average over the average Atlantic water extent, Eq. (7) explains 48 % of the total variance in the observed salinity (Hansen et al., 2015, Fig. 4.8.2).

3.3 Volume transport

3.3.1 Total volume transport

Once appropriate choices for the relative profile functions $\varphi_k(z, t)$ and $\Phi_k(z)$ have been made for each altimetry interval k (Hansen et al., 2015, Table 5.3.1), Eqs. (1) to (3) allow calculation of volume transport, as long as the $W_k(z, t)$ functions are specified. As a test case, we consider the volume transport from the surface to 500 m and from N02 (midway between A_2 and A_3) out to A_8 (Fig. 1b), which we here denote total volume

Title Page

Abstract

Introduction

Conclusions

References

Tables

Figures

|◀

▶|

◀

▶

Back

Close

Full Screen / Esc

Printer-friendly Version

Interactive Discussion



Increasing transports of volume, heat, and salt towards the Arctic in the Faroe Current 1993–2013

B. Hansen et al.

[Title Page](#)

[Abstract](#)

[Introduction](#)

[Conclusions](#)

[References](#)

[Tables](#)

[Figures](#)

[◀](#)

[▶](#)

[◀](#)

[▶](#)

[Back](#)

[Close](#)

[Full Screen / Esc](#)

[Printer-friendly Version](#)

[Interactive Discussion](#)



transport. This requires $W_2(z, t) = L/2$ and $W_k(z, t) = L$ for $k = 3$ to 7 for all depths $z = 1$ to 500 (or bottom where shallower). Outside of this area $W_k(z, t) = 0$.

From 1 January 1993 to 1 May 2014, there are 223 weeks for which we have altimetry data, as well as data from all four long-term ADCP sites (NA, NE, NB, and NG). For these weeks, we can compare transport estimates based on the instantaneous relative profiles $\varphi_k(z, t)$ with estimates based on the average relative profiles $\Phi_k(z)$. For weekly averages, the correlation coefficient between these two estimates is 0.92 with an average difference of 0.06 Sv and a rms (root-mean-square) difference of 0.4 Sv, which is 9 % of the average (Hansen et al., 2015, Table 5.3.2 and Fig. 5.3.1). For 4 week averages, the comparison is even better.

This implies that the average relative profiles $\Phi_k(z)$ may be used instead of $\varphi_k(z, t)$ without appreciable error. More importantly, it implies that the $\Phi_k(z)$ functions, which do not depend upon time, give a sufficiently good representation of the velocity variation, vertically, to allow accurate transport calculation whenever the surface velocity is known. As a consequence, we can calculate transports; not only for periods with good ADCP coverage, but for the whole altimetry period since 1 January 1993.

3.3.2 Volume transport of Atlantic water

The total volume transport down to 500 m depth, calculated above, includes water of Arctic origin. To obtain an estimate of Atlantic water volume transport only, values for $W_k(z, t)$ have to be specified, so that the transport estimate only includes water that has crossed the IFR recently. One way to do that is to assume that the Atlantic water on the section is bounded by a specified isotherm or isohaline. Table 2 compares volume transports using different choices for the bounding isoline and assuming that it remains fixed to its average depth.

In reality, the isolines do not stay at fixed depths and the deep boundary of the Atlantic water extent, as well as its northward surface boundary, vary in time. We use the 4 °C isotherm (or bottom where shallower) to define the deep boundary and the 35.0 isohaline to define the northward boundary in the 0 to 100 m depth layer. Both of

Title Page	
Abstract	Introduction
Conclusions	References
Tables	Figures
◀	▶
◀	▶
Back	Close
Full Screen / Esc	
Printer-friendly Version	
Interactive Discussion	

these may be simulated for each day in the altimetry period, as discussed in Sect. 3.2.2 (Hansen et al., 2015, Table 4.2.2 and Eq. 4.4.2), allowing daily estimates of $W_k(z, t)$.

The data set, thus, allows daily estimates of Atlantic water volume transport, but the algorithms are developed from regression analyses, that will give better estimates for longer averaging periods. Also, we expect the quality of the altimetry data, and even the validity of geostrophy, to increase with the averaging period. In the following, we therefore will consider monthly averaged transport values.

To study the variations in Atlantic water volume transport, monthly averages were calculated for the 1993 to 2013 period. The overall average was 3.82 Sv and an iterative procedure (Hansen et al., 2015, Appendix B) was used to extract seasonal (Fig. 6a) and long-term (Fig. 6b) variations. In contrast to previous studies (Hansen et al., 2003, 2010), there is an indication of a seasonal variation with maximum flow around the turn of the year. The maximum correlation coefficient in the fit with the sinusoidal signal was, however, not very high and the seasonal amplitude was below 10 % of the average (Table 3). On average, more than 70 % of the Atlantic water transport occurs between A_3 and A_5 (Hansen et al., 2015, Fig. 5.4.1).

As previously noted (Hansen et al., 2010), the annually averaged Atlantic water volume transport had a minimum in 2003, but since then, it seems to have been at a generally higher level than before 2003 (Fig. 6b). A linear regression on time reveals an increasing trend: $0.016 \pm 0.015 \text{ Sv yr}^{-1}$ with a 95 % confidence interval (Table 3).

3.4 Heat transport

The heat delivered by any inflow branch to the Arctic Mediterranean (Nordic Seas and Arctic Ocean) depends on the temperature of the water when it returns back to the Atlantic Ocean, either as overflow, or as surface outflow in the East Greenland Current or through the Canadian Archipelago. Thus, the heat transport of the Faroe Current is only well defined if we know the average outflow temperature, which is the appropriate *reference temperature*, T_{Ref} in Eq. (4). The detailed pathways of the various inflow branches are not well known, but most likely the average outflow temperature of the

**Increasing transports
of volume, heat, and
salt towards the
Arctic in the Faroe
Current 1993–2013**

B. Hansen et al.

water that entered in the Faroe Current is close to 0 °C (Hansen et al., 2008). We therefore calculate heat transport relative to $T_{\text{Ref}} = 0$ °C and term this *relative heat transport*.

As noted in Sect. 3.2.3, we may simulate daily temperature fields $T_j(z, t)$ for the whole altimetry period with reasonable accuracy. This allows us to use Eq. (4) to calculate relative heat transport, but it is not obvious that the 4 °C isotherm is the appropriate boundary in this case, since the Atlantic water that by mixing has been cooled below 4 °C originally carried more heat than the Arctic water that has been heated above 4 °C. Instead, we should use a colder isotherm as Atlantic water boundary for heat transport calculation. The cold waters close to the Atlantic water boundary do, however, not transport much heat, especially since average velocities are low. Consistent with that, we also find that the average relative heat transport is not very sensitive to the exact definition of Atlantic water extent (Hansen et al., 2015, Table 6.1.1).

As for the volume transport, the relative heat transport does not exhibit a very pronounced seasonal variation (Hansen et al., 2015, Fig. 6.1.2), and the seasonal amplitude is about 10 % of the average (Table 3). For the long-term variation, Fig. 7 clearly indicates an increasing trend, which is $1.0 \pm 0.5 \text{ TW yr}^{-1}$, from a linear regression on time. This is highly significant and not very dependent on the boundary chosen for Atlantic water extent (Hansen et al., 2015, Table 6.1.1). Over the 20 year interval from 1993 to 2013, this corresponds to an increase in relative heat transport of ~18 %. Most of the change occurred from 2003 to 2006.

3.5 Salt transport

The salt transport through section N by Atlantic water is given by Eq. (5). Eventually, this salt is returned to the Atlantic by the overflows and surface outflows, but the returning water has been diluted by added freshwater and the low-salinity Pacific inflow through the Bering Strait. A rough budget estimate indicates that the salinity is reduced by about 1 on average (Hansen et al., 2008), but the overflows, which will return a large fraction of the Faroe Current, are more saline. The average salinity of the neighbouring (Fig. 1a) Faroe Bank Channel overflow is ~34.93 (Hansen and Østerhus, 2007).

Title Page	
Abstract	Introduction
Conclusions	References
Tables	Figures
◀	▶
◀	▶
Back	Close
Full Screen / Esc	
Printer-friendly Version	
Interactive Discussion	

	Title Page
	Abstract
	Introduction
	Conclusions
	References
	Tables
	Figures
◀	▶
◀	▶
Back	Close
	Full Screen / Esc
	Printer-friendly Version
	Interactive Discussion

In addition to the absolute salt transport, which we get by choosing the *reference salinity* $S_{\text{Ref}} = 0$, it may therefore be appropriate to consider the transport relative to some other values for S_{Ref} . Using the simulated values for $S_j(z, t)$ in Eq. (7), time series of salt transport for specified values of S_{Ref} may be generated, but the problem, again, is to distinguish between the Atlantic water and other water masses. This introduces considerable uncertainty into calculations of absolute salt transport, but the salt transport relative to higher salinities is much less sensitive to the boundary chosen for Atlantic water extent (Hansen et al., 2015, Table 6.2.1). This is reflected in the uncertainties for the average values listed in Table 3.

As for volume and relative heat transport, we can extract the seasonal (Table 3) and a long-term variation (Hansen et al., 2015, Appendix B) from the salt transport time series. This clearly has an increasing trend whether we consider the absolute transport ($S_{\text{Ref}} = 0$), or the transport relative to 34.93 (Fig. 8). A linear regression of annually averaged salt transport on time yields trends that are positive and significantly different from zero for all choices of S_{Ref} (Hansen et al., 2015, Table 6.2.1) and more significant, the higher the S_{Ref} value. The salt transport relative to $S_{\text{ref}} = 34.93$ more than doubled throughout the observational period (Fig. 8).

3.6 Uncertainty estimates

Many different approximations affect the accuracies of the average transport values reported here and fully objective error estimates are difficult to generate from the available information. Combining the contributions from various error sources, we estimate an uncertainty 0.5 Sv for the average Atlantic water volume transport and 15 TW for the average relative heat transport (Hansen et al., 2015, Chapter 7). For salt transport, the uncertainties depend greatly on the choices of reference salinity.

For our purpose, the most important question is the reliability of the trends that we find for the transport series of volume, heat and salt. For these trends, most of the error sources for the average values cancel out and the rest should be included in the statistical error bounds reported for the trends except for possible systematic errors

in the altimetry data. If these data were to include artificial long-term trends, then the trend in volume transport might be affected, but the trends in relative heat and salt transport would still be robust since they are dominated by the trends in Atlantic water temperature and salinity (Fig. 5).

5 4 Discussion

The transport time series presented in this study are generated from a number of assumptions and approximations: geostrophy, use of the average relative profiles $\Phi_k(z)$ in Eq. (2), our choice of the 4 °C isotherm and 35.0 isohaline as boundaries for Atlantic water extent, etc. Based on an evaluation of their effects on the results, we find that the 10 chosen method of combining in situ observations with altimetry produces more reliable transport values than estimates based on the in situ data, solely (Hansen et al., 2015, Chapter 8). We also find that the method allows estimates in periods without in situ velocity measurements as long as there are no major changes in the structure of the 15 velocity field. This justifies the validity of our continuous transport series for the whole altimetry period.

4.1 Comparison with other estimates of the IF-inflow

The overall average Atlantic water transport for 1993–2013, estimated in this study (3.8 ± 0.5 Sv) is slightly higher than the previously reported average transport (3.5 ± 0.5 Sv), based on a subset of the same in situ data, but without using altimetry data 20 (Hansen et al., 2003, 2010). The difference is within the uncertainty bounds, however. Comparing monthly averaged volume transport estimates, the best correspondence is for the 57 months when all four long-term ADCPs were in operation (Hansen et al., 2015, Fig. 5.5.1), but even in that case the correlation coefficient is only 0.58 (Hansen et al., 2015, Table 5.5.1). Considering the approximations made in the old in situ based

OSD

12, 1013–1050, 2015

Increasing transports
of volume, heat, and
salt towards the
Arctic in the Faroe
Current 1993–2013

B. Hansen et al.

Title Page	
Abstract	Introduction
Conclusions	References
Tables	Figures
◀	▶
◀	▶
Back	Close
Full Screen / Esc	
Printer-friendly Version	
Interactive Discussion	

**Increasing transports
of volume, heat, and
salt towards the
Arctic in the Faroe
Current 1993–2013**

B. Hansen et al.

estimates, we conclude, however, that the new transport values should be more realistic than the old ones (Hansen et al., 2015, Sect. 5.5).

In addition to our own old estimates, there are not many observational transport estimates of the IF-inflow, but Rossby and Flagg (2012) and Childers et al. (2014) have reported estimates based mainly on vessel-mounted ADCP observations from a ferry making regular tracks between Faroes and eastern Iceland. Differences in definitions and timing make detailed comparisons difficult, but their average transport values are so much higher than ours that they are difficult to reconcile.

Transport values for the IF-inflow have also been estimated by ocean models, but even with relatively high resolution (e.g., Sandø et al., 2012), the flow over the complicated topography of the IFR remains challenging to model and Olsen et al. (2015) have argued that feedback mechanisms between the IF-inflow and the IF-overflow make it difficult to disentangle the IF-inflow from the net flow across the IFR (IF-inflow minus IF-overflow).

4.2 The Faroe Current in a climate perspective

The inflow of Atlantic water to the Nordic Seas plays two main roles in the climate system: (1) it transports heat into the Arctic Mediterranean, which affects sea ice and marine conditions, as well as the climate of the surrounding land masses, and (2) it transports salt into the region, which is a precondition for the thermohaline ventilation and hence the circulation system both locally and more globally through the North Atlantic THC.

In the literature, the Atlantic inflow is traditionally split into three separate branches (e.g., Østerhus et al., 2005) and average transport values have been reported for the branch west of Iceland (the North Icelandic Irminger Current) by Jónsson and Valdimarsson (2012) and for the flow through the Faroe–Shetland Channel by Berx et al. (2013). When these values are compared with our results (Table 4), the Faroe Current is found to carry more than 50 % of the total volume transport and 48 % of the total heat transport relative to 0 °C.

[Title Page](#)[Abstract](#)[Introduction](#)[Conclusions](#)[References](#)[Tables](#)[Figures](#)[|◀](#)[▶|](#)[◀](#)[▶](#)[Back](#)[Close](#)[Full Screen / Esc](#)[Printer-friendly Version](#)[Interactive Discussion](#)

This comparison does not take into account the flow of Atlantic water over the shelf region between the Faroe–Shetland Channel and the European continent through various passages including the English Channel. We have no reliable estimate of the combined transports associated with this flow, but the scant observational evidence (Turrell et al., 1990; Childers et al., 2014; Prandle, 1996) indicates that it is well below 1 Sv.

When considering the whole Arctic Mediterranean, we also need to include the inflow through the Bering Strait, where the volume transport increased from 0.7 to 1.1 Sv between 2001 and 2011. The temperature of the Bering Strait inflow is low, however, and its heat transport does not exceed 20 TW (Woodgate et al., 2012).

The Faroe Current, thus remains the dominant inflow branch to the Arctic Mediterranean and its heat transport is likely more than one third of the total oceanic heat import to the area. Our observation of an 18 % increase during the two decades of observation therefore represents a significant increase in the total oceanic heat import. The two other branches in Table 4 have also experienced increasing temperatures since the mid-1990s (Jónsson and Valdimarsson, 2012; Berx et al., 2013) and it seems likely that their heat transports have increased as well, although the high variability of the transports of these branches makes statistically significant trends difficult to identify.

A discussion on the consequences of increased heat transport is not within the scope of this paper, but we note that oceanic heat transport has been linked to sea ice reduction in the Barents Sea (Årthun et al., 2012) and north of Svalbard (Onarheim et al., 2014) farther downstream on the path of the Atlantic inflow. In the Arctic Ocean, the submerged Atlantic water is partly isolated from the surface by the halocline, but Rippeith et al. (2015) have demonstrated enhanced vertical mixing over steep topography, allowing more heat from the Atlantic layer to reach the surface. On its way northwards, the heat carried by the Atlantic inflow also tends to warm the ambient waters (Mork et al., 2014) and enable pelagic fish species to use a larger part of the Norwegian Sea during the feeding period with huge economical perspectives (Utne et al., 2012).

Increasing transports of volume, heat, and salt towards the Arctic in the Faroe Current 1993–2013

B. Hansen et al.

[Title Page](#)

[Abstract](#)

[Introduction](#)

[Conclusions](#)

[References](#)

[Tables](#)

[Figures](#)

[◀](#)

[▶](#)

[◀](#)

[▶](#)

[Back](#)

[Close](#)

[Full Screen / Esc](#)

[Printer-friendly Version](#)

[Interactive Discussion](#)



**Increasing transports
of volume, heat, and
salt towards the
Arctic in the Faroe
Current 1993–2013**

B. Hansen et al.

[Title Page](#)[Abstract](#)[Introduction](#)[Conclusions](#)[References](#)[Tables](#)[Figures](#)[|◀](#)[▶|](#)[◀](#)[▶](#)[Back](#)[Close](#)[Full Screen / Esc](#)[Printer-friendly Version](#)[Interactive Discussion](#)

The increased heat transport of the Faroe Current stems partly from the increased temperature of the Atlantic water (Fig. 5) and partly from the increased volume transport (Fig. 6b). The temperature increase mainly occurred from the mid-1990s to 2003, which has been ascribed to a weakening of the subpolar gyre (Häkkinen and Rhines, 5 2004; Hátún et al., 2005). Later variations in the Atlantic water temperature seem more affected by regional air–sea interaction (Larsen et al., 2012).

The increased volume transport is notable in view of the projected decline of the Atlantic Meridional Overturning Circulation, AMOC (Collins et al., 2013), which is fed by two North Atlantic THC sources, a western (Labrador Sea) and an eastern (Arctic 10 Mediterranean) source (Hansen et al., 2004). It has been suggested that the changes observed in the western North Atlantic may indicate a weakening in that THC source (Robson et al., 2014; Rahmstorf et al., 2015). The main branches of the eastern THC component (Nordic Seas – Arctic Ocean) have been monitored since the mid-1990s, but there we find no convincing evidence for a weakening.

15 The deep branch of the eastern THC component is dominated by the two main overflows: through the Denmark Strait and through the Faroe Bank Channel. In the Denmark Strait, Jochumsen et al. (2012, 2015) report no significant long-term trend and in the Faroe Bank Channel (Hansen and Østerhus, 2007 updated with unpublished data), there has been a slightly increasing trend from 1996 to 2014, although not statistically 20 significant.

The picture is very similar for the upper branch. The inflow branch through the Faroe–Shetland Channel does not show any significant trend (Berx et al., 2013). For the inflow west of Iceland, there are indications of an increasing trend (Jónsson and Valdimars- 25 son, 2012) and Fig. 6b indicates the same for the Faroe Current. It remains to be seen whether these trends will persist.

In this regard, the salt transport is of interest because it may act as a positive feedback on the circulation (Stommel, 1961; Latif et al., 2000). In Table 4, we have not included salt transports; mainly because their values depend critically on the rather ad hoc choice of reference salinity. Regardless of this choice, the salt transport of the

Faroe Current has experienced a highly significant increasing trend (Table 3). With reference to the average salinity (34.93) of the Faroe Bank Channel overflow (Hansen and Østerhus, 2007), the salt transport more than doubled from 1993 to 2013 (Fig. 8).

The sensitivity of the THC to freshwater anomalies has been widely studied in modelling experiments, but Glessmer et al. (2014) have recently shown that freshwater anomalies in the Nordic Seas are mainly of Atlantic, rather than Arctic, origin. This highlights the importance of the salt transport by the Atlantic inflow and the large increase that we have observed in the Faroe Current should act to stimulate the overflows and thereby also the Faroe Current itself (Hansen et al., 2010). Whether, this has played any role in the observed strengthening of the Faroe Current (Fig. 6b), remains to be seen.

5 Conclusions

The method used in this study, combining altimetry and in situ observations, has weaknesses, but is found to give more reliable transport estimates than the previously used method based solely on in situ data. This also allows transport estimates for the whole altimetry period, from 1 January 1993, including periods with no in situ current measurements.

Average values for volume and heat (relative to 0 °C) transports of Atlantic water in the Faroe Current were found to be 3.8 ± 0.5 Sv and 124 ± 15 TW, respectively. The average salt transport depends on the choice of reference salinity. All the transports had a seasonal variation with maximum between October and January, although the seasonal amplitudes were only ~ 10 % of the averages and not very persistent. All the transports also increased during the 1993 to 2013 period. From the trend analysis, percentage (relative to the beginning) annual increases were $0.4 \pm 0.4\% \text{ yr}^{-1}$ for the volume transport and $0.9 \pm 0.4\% \text{ yr}^{-1}$ for heat transport relative to 0 °C. For the absolute salt transport (relative to salinity 0), the annual increase was $2.2 \pm 0.8\% \text{ yr}^{-1}$, whereas the salt transport relative to 34.93 increased by $6 \pm 1\% \text{ yr}^{-1}$.

[Title Page](#)[Abstract](#)[Introduction](#)[Conclusions](#)[References](#)[Tables](#)[Figures](#)[◀](#)[▶](#)[Back](#)[Close](#)[Full Screen / Esc](#)[Printer-friendly Version](#)[Interactive Discussion](#)

Acknowledgements. The authors wish to thank captains and crew on the R/V *Magnus Heinason* for unfailing support during measurements at sea. Funding for the in situ measurements has been obtained from the Environmental Research Programme of the Nordic Council of Ministers (NMR) 1993–1998, from national Nordic research councils, from the Danish DANCEA programme, and from the European Framework Programs, lately under grant agreement No. GA212643 (THOR) and under grant agreement No. 308299 (NACLIM). Analysis and preparation of this manuscript was mainly funded by the NACLIM project and by the Danish Strategic Research Program through the NAACOS project.

References

- Årthun, M., Eldevik, T., Smedsrød, L. H., Skagseth, Ø., and Ingvaldsen, R. B.: Quantifying the influence of Atlantic heat on Barents Sea ice variability and retreat, *J. Climate*, 25, 4736–4743, doi:10.1175/JCLI-D-11-00466.1, 2012.
- Berx, B., Hansen, B., Østerhus, S., Larsen, K. M., Sherwin, T., and Jochumsen, K.: Combining in situ measurements and altimetry to estimate volume, heat and salt transport variability through the Faroe–Shetland Channel, *Ocean Sci.*, 9, 639–654, doi:10.5194/os-9-639-2013, 2013.
- Childers, K. H., Flagg, C. N., and Rossby, T.: Direct velocity observations of volume flux between Iceland and the Shetland Islands, *J. Geophys. Res.-Oceans*, 119, 5934–5944, doi:10.1002/2014JC009946, 2014.
- Collins, M., Knutti, R., Arblaster, J., Dufresne, J.-L., Fichefet, T., Friedlingstein, P., Gao, X., Gutowski, W. J., Johns, T., Krinner, G., Shongwe, N., Tebaldi, C., Weaver, A. J., and Wehner, M.: Long-term climate change: projections, commitments and irreversibility, Chap. 12, in: *Climate Change 2013: the Physical Science Basis. Contribution of Working Group I to the Fifth Assessment Report of the Intergovernmental Panel on Climate Change*, edited by: Stocker, T. F., Qin, D., Plattner, G.-K., Tignor, M., Allen, S. K., Boschung, J., Nauels, A., Xia, Y., Bex, V., and Midgley, P. M., Cambridge University Press, Cambridge, UK, New York, NY, USA, 2013.
- Glessmer, M. S., Eldevik, T., Våge, K., Nilsen, J. E. O., and Behrens, E.: Atlantic origin of observed and modelled freshwater anomalies in the Nordic Seas, *Nat. Geosci.*, 7, 801–805, doi:10.1038/NGEO2259, 2014.

[Title Page](#)[Abstract](#)[Introduction](#)[Conclusions](#)[References](#)[Tables](#)[Figures](#)[◀](#)[▶](#)[Back](#)[Close](#)[Full Screen / Esc](#)[Printer-friendly Version](#)[Interactive Discussion](#)

**Increasing transports
of volume, heat, and
salt towards the
Arctic in the Faroe
Current 1993–2013**

B. Hansen et al.

- Hansen, B. and Østerhus, S.: Faroe Bank Channel overflow 1995–2005, *Prog. Oceanogr.*, 75, 817–856, doi:10.1016/j.pocean.2007.09.004, 2007.
- Hansen, B., Østerhus, S., Hátún, H., Kristiansen, R., and Larsen, K. M. H.: The Iceland–Faroe inflow of Atlantic water to the Nordic Seas, *Prog. Oceanogr.*, 59, 443–474, doi:10.1016/j.pocean.2003.10.003, 2003.
- Hansen, B., Østerhus, S., Quadfasel, D., and Turrell, W.: Already the day after tomorrow?, *Science*, 305, 953–954, 2004.
- Hansen, B., Østerhus, S., Turrell, W. R., Jónsson, S., Valdimarsson, H., Hátún, H., and Olsen, S. M.: The inflow of Atlantic water, heat, and salt to the Nordic Seas across the Greenland–Scotland Ridge, Chap. 1, in: Arctic–Subarctic Ocean Fluxes: Defining the Role of the Northern Seas in Climate, edited by: Dickson, R. R., Meincke, J., and Rhines, P., Springer Science + Business Media B. V., 15–43, 2008.
- Hansen, B., Hátún, H., Kristiansen, R., Olsen, S. M., and Østerhus, S.: Stability and forcing of the Iceland–Faroe inflow of water, heat, and salt to the Arctic, *Ocean Sci.*, 6, 1013–1026, doi:10.5194/os-6-1013-2010, 2010.
- Hansen, B., Larsen, K. M. H., Hátún, H., Kristiansen, R., Mortensen, E., and Østerhus, S.: Monitoring volume, heat, and salt transports in the Faroe Current 1993–2013, Faroe Marine Research Institute Technical Report No. 15-01, 53 pp., available at: www.hav.fo/PDF/Ritgerdir/2015/TecRep1501.pdf, 2015.
- Hátún, H. and McClimans, T. A.: Monitoring the Faroe Current using altimetry and coastal sea-level data, *Cont. Shelf Res.*, 23, 859–868, doi:10.1016/S0278-4343(03)00059-1, 2003.
- Hátún, H., Hansen, B., and Haugan, P.: Using an “inverse dynamic method” to determine temperature and salinity fields from ADCP measurements, *J. Atmos. Ocean. Tech.*, 21, 527–534, 2004.
- Hátún, H., Sandø, A. B., Drange, H., Hansen, B., and Valdimarsson, H.: Influence of the Atlantic subpolar gyre on the thermohaline circulation, *Science*, 309, 1841–1844, 2005.
- Häkkinen, S. and Rhines, P. B.: Decline of subpolar North Atlantic circulation during the 1990s, *Science*, 304, 555–559, 2004.
- Jakobsen, P. K., Ribergaard, M. H., Quadfasel, D., Schmitt, T., and Hughes, C. W.: Near-surface circulation in the northern North Atlantic as inferred from Lagrangian drifters: variability from the mesoscale to interannual, *J. Geophys. Res.-Oceans*, 108, 3251, doi:10.1029/2002JC001554, 2003.

[Title Page](#)[Abstract](#)[Introduction](#)[Conclusions](#)[References](#)[Tables](#)[Figures](#)[|◀](#)[▶|](#)[◀](#)[▶](#)[Back](#)[Close](#)[Full Screen / Esc](#)[Printer-friendly Version](#)[Interactive Discussion](#)

Increasing transports of volume, heat, and salt towards the Arctic in the Faroe Current 1993–2013

B. Hansen et al.

- Jochumsen, K., Quadfasel, D., Valdimarsson, H., and Jonsson, S.: Variability of the Denmark Strait overflow: moored time series from 1996–2011, *J. Geophys. Res.-Oceans*, 117, C12003, doi:10.1029/2012JC008244, 2012.
- Jochumsen, K., Köllner, M., Quadfasel, D., Dye, S., Rudels, B., and Valdimarsson, H.: On the origin and propagation of Denmark Strait overflow water anomalies in the Irminger Basin, *J. Geophys. Res.-Oceans*, 120, 1841–1855, doi:10.1002/2014JC010397, 2015.
- Jónsson, S. and Valdimarsson, H.: Water mass transport variability to the North Icelandic shelf, 1994–2010, *ICES J. Mar. Sci.*, 69, 809–815, doi:10.1093/icesjms/fss024, 2012.
- Larsen, K. M. H., Hátún, H., Hansen, B., and Kristiansen, R.: Atlantic water in the Faroe area: sources and variability, *ICES J. Mar. Sci.*, 69, 802–808, doi:10.1093/icesjms/fss028, 2012.
- Latif, M., Roeckner, E., Mikolajewicz, U., and Voss, R.: Tropical stabilization of the thermohaline circulation in a greenhouse warming simulation, *J. Climate*, 13, 1809–1813, 2000.
- Mork, K. A., Skagseth, Ø., Ivshin, V., Ozhigin, V., Hughes, S. L., and Valdimarsson, H.: Advection and atmospheric forced changes in heat and freshwater content in the Norwegian Sea, 1951–2010, *Geophys. Res. Lett.*, 41, 6221–6228, doi:10.1002/2014GL061038, 2014.
- Olsen, S. M., Hansen, B., Østerhus, S., Quadfasel, D., and Valdimarsson, H.: Biased thermo-haline exchanges with the arctic across the Iceland–Faroe Ridge in ocean climate models, *Ocean Sci. Discuss.*, submitted, 2015.
- Onarheim, I. H., Smetsrud, L. H., Ingvaldsen, R. B., and Nilsen, F.: Loss of sea ice during winter north of Svalbard, *Tellus A*, 66, 23933, doi:10.3402/tellusa.v66.23933, 2014.
- Orvik, K. A. and Niiler, P.: Major pathways of Atlantic water in the northern North Atlantic and Nordic Seas toward Arctic, *Geophys. Res. Lett.*, 29, 1896, doi:10.1029/2002GL015002, 2002.
- Østerhus, S., Turrell, W. R., Jónsson, S., and Hansen, B.: Measured volume, heat, and salt fluxes from the Atlantic to the Arctic Mediterranean, *Geophys. Res. Lett.*, 32, L07603, doi:10.1029/2004GL022188, 2005.
- Prandle, D., Ballard, G., Flatt, D., Harrison, A. J., Jones, S. E., Knight, P. J., Loch, S., Manus, J., Player, R., and Tappin, A.: Combining modelling and monitoring to determine fluxes of water, dissolved and particulate metals through the Dover Strait, *Cont. Shelf Res.*, 16, 237–257, 1996.
- Rahmstorf, S., Box, J. E., Feulner, G., Mann, M. E., Robinson, A., Rutherford, S., and Schaffernicht, E. J.: Exceptional twentieth-century slowdown in Atlantic Ocean overturning circulation, *Nat. Clim. Change*, 5, 475–480, doi:10.1038/nclimate2554, 2015.

[Title Page](#)

[Abstract](#)

[Introduction](#)

[Conclusions](#)

[References](#)

[Tables](#)

[Figures](#)

[◀](#)

[▶](#)

[Back](#)

[Close](#)

[Full Screen / Esc](#)

[Printer-friendly Version](#)

[Interactive Discussion](#)



**Increasing transports
of volume, heat, and
salt towards the
Arctic in the Faroe
Current 1993–2013**

B. Hansen et al.

- Rippeth, T. P., Lincoln, B. J., Lenn, Y.-D., Green, J. A. M., Sundfjord, A., and Bacon, S.: Tide-mediated warming of Arctic halocline by Atlantic heat fluxes over rough topography, *Nat. Geosci.*, 8, 191–194, doi:10.1038/NGEO2350, 2015.
- Robson, J., Hodson, D., Hawkins, E., and Sutton, R.: Atlantic overturning in decline?, *Nat. Geosci.*, 7, 2–3, 2014.
- Rossby, T. and Flagg, C. N.: Direct measurement of volume flux in the Faroe–Shetland Channel and over the Iceland–Faroe Ridge, *Geophys. Res. Lett.*, 39, L07602, doi:10.1029/2012GL051269, 2012.
- Rossby, T., Prater, M. D., and Søiland, H.: Pathways of inflow and dispersion of warm waters in the Nordic seas, *J. Geophys. Res.-Oceans*, 114, C04011, doi:10.1029/2008JC005073, 2009.
- Sandø, A. B., Nilsen, J. E. O., Eldevik, T., and Bentsen, M.: Mechanisms for variable North Atlantic-Nordic seas exchanges, *J. Geophys. Res.-Oceans*, 117, C12006, doi:10.1029/2012JC008177, 2012.
- Stommel, H.: Thermohaline convection with two stable regimes of flow, *Tellus*, 13, 224–230, 1961.
- Turrell, W. R., Henderson, E. W., and Slesser, G.: Residual transport within the fair isle current observed during the Autumn Circulation Experiment (ACE), *Cont. Shelf Res.*, 10, 521–543, 1990.
- Utne, K. R., Huse, G., Ottersen, G., Holst, J. C., Zabavnikov, V., Jacobsen, J. A., Oskarsdóttir, G. J., and Nøttestad, L.: Horizontal distribution and overlap of planktivorous fish stocks in the Norwegian Sea during summers 1995–2006, *Mar. Biol. Res.*, 8, 420–441, 2012.
- Woodgate, R. A., Weingartner, T. J., and Lindsay, R.: Observed increases in Bering Strait oceanic fluxes from the Pacific to the Arctic from 2001 to 2011 and their impacts on the Arctic Ocean water column, *Geophys. Res. Lett.*, 39, L24603, doi:10.1029/2012GL054092, 2012.

[Title Page](#)[Abstract](#)[Introduction](#)[Conclusions](#)[References](#)[Tables](#)[Figures](#)[|◀](#)[▶|](#)[Back](#)[Close](#)[Full Screen / Esc](#)[Printer-friendly Version](#)[Interactive Discussion](#)

Increasing transports of volume, heat, and salt towards the Arctic in the Faroe Current 1993–2013

B. Hansen et al.

Table 1. Main characteristics of the measurements at the seven ADCP sites. “Depth” is the bottom depth at the site and “Days” is the number of days of observation. For the four long-term deployment sites, the table also lists averages (“Av”, in cm s^{-1}), and standard deviations (“Sd”, in cm s^{-1}) of the extrapolated eastward surface velocity.

Site	Latitude	Depth	Period	Days	Av	Sd
NA	62.70° N	300	Jan 1996–May 2014	6311	18	15
NE	62.79° N	455	Jul 2000–May 2011	2729	25	19
NB	62.92° N	925	Jun 1997–May 2014	5775	22	20
NG	63.10° N	1815	Jul 2000–May 2014	4436	12	21
NF	62.88° N	700	Jul 2000–Jun 2001	343		
ND	62.96° N	1280	Nov 1997–Jun 1998	213		
NC	63.27° N	1730	Jun 1996–Jun 2000	1400		

**Increasing transports
of volume, heat, and
salt towards the
Arctic in the Faroe
Current 1993–2013**

B. Hansen et al.

Table 2. Average (1 January 1993 to 1 May 2014) volume transport between N02 and A_g above either a fixed depth of 500 m, a selected average isotherm ($T =$), or a selected average isohaline ($S =$) in the hydrographic fields.

Isoline:	$D = 500\text{ m}$	$T = 2^\circ\text{C}$	$T = 3^\circ\text{C}$	$T = 4^\circ\text{C}$	$T = 5^\circ\text{C}$	$T = 6^\circ\text{C}$	$T = 7^\circ\text{C}$	$S = 34.9$	$S = 35.0$	$S = 35.1$
Transport (Sv):	4.66	4.46	4.28	4.05	3.76	3.35	2.70	4.56	3.95	3.26

[Title Page](#)[Abstract](#)[Introduction](#)[Conclusions](#)[References](#)[Tables](#)[Figures](#)[|◀](#)[▶|](#)[◀](#)[▶](#)[Back](#)[Close](#)[Full Screen / Esc](#)[Printer-friendly Version](#)[Interactive Discussion](#)

Increasing transports of volume, heat, and salt towards the Arctic in the Faroe Current 1993–2013

B. Hansen et al.

Table 3. Characteristics of transport time series. Averages for the 1993 to 2013 period. Trends are based on a linear regression of annual averages on time with 95 % confidence intervals. Seasonal variation is determined by an iterative procedure (Hansen et al., 2015, Appendix B) where “ R_{\max} ” is the maximum correlation coefficient with a sinusoidal seasonal signal, “Ampl.” is the seasonal amplitude and “Max.” is the day number in the year with maximum value.

Time series	Average	Trend	Seasonal variation		
			R_{\max}	Ampl.	Max.
Atlantic water volume transport:	3.8 ± 0.5 Sv	0.016 ± 0.015 Sv yr^{-1}	0.34	0.34 Sv	1
Heat transport relative to 0°C:	124 ± 15 TW	1.0 ± 0.5 TW yr^{-1}	0.39	13 TW	307
Absolute salt transport:	$(140 \pm 30) \times 10^6$ kgs^{-1}	$(1.9 \pm 0.7) \times 10^6$ $\text{kgs}^{-1} \text{yr}^{-1}$	0.33	14×10^6 kgs^{-1}	14
Salt transport relative to 34.93:	$(900 \pm 140) \times 10^3$ kgs^{-1}	$(33 \pm 7) \times 10^3$ $\text{kgs}^{-1} \text{yr}^{-1}$	0.33	91×10^3 kgs^{-1}	352

Title Page

Abstract

Introduction

Conclusions

References

Tables

Figures

◀

▶

Back

Close

Full Screen / Esc

Printer-friendly Version

Interactive Discussion



**Increasing transports
of volume, heat, and
salt towards the
Arctic in the Faroe
Current 1993–2013**

B. Hansen et al.

Table 4. Average volume and heat (relative to 0 °C) transport in the three Atlantic inflow branches for the period 1995 to 2009 (for the branch west of Iceland, the period is 1994 to 2010).

Inflow branch	Vol. transp.	Heat transp.
West of Iceland:	0.9 ± 0.1 Sv	24 ± 4 TW
Faroe Current:	3.8 ± 0.5 Sv	123 ± 15 TW
Faroe–Shetland Channel:	2.7 ± 0.5 Sv	107 ± 21 TW

[Title Page](#)[Abstract](#)[Introduction](#)[Conclusions](#)[References](#)[Tables](#)[Figures](#)[|◀](#)[▶|](#)[◀](#)[▶](#)[Back](#)[Close](#)[Full Screen / Esc](#)[Printer-friendly Version](#)[Interactive Discussion](#)

Increasing transports of volume, heat, and salt towards the Arctic in the Faroe Current 1993–2013

B. Hansen et al.

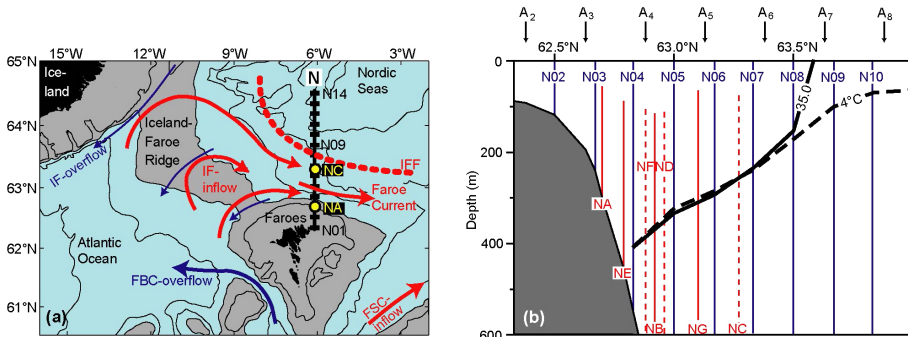


Figure 1. (a) The region between Iceland and the Scottish shelf with grey areas shallower than 500 m. The two main Atlantic inflow branches are indicated by red arrows. The Iceland–Faroe inflow (IF-inflow) crosses the IFR, meets colder waters, termed Arctic water, in the Iceland–Faroe Front (IFF), and flows north of Faroes in the Faroe Current. The black line extending northwards from the Faroe shelf is section N with CTD standard stations N01 to N14 indicated by black rectangles. Yellow circles indicate the innermost (NA) and the outermost (NC) ADCP mooring sites on the section. Blue arrows indicate deep overflow into the Atlantic. (b) The southernmost part of section N with bottom topography (grey). Standard CTD stations are indicated by blue lines labeled N02 to N10. ADCP profiles are marked by red lines that indicate the typical range with continuous lines indicating the long-term sites. Altimetry grid points A₂ to A₈ are marked by black arrows and the thick black lines indicate the average depth of the 4°C isotherm (dashed) and the 35.0 isohaline (continuous) on the section.

Title Page	
Abstract	Introduction
Conclusions	References
Tables	Figures

◀	▶
◀	▶
Back	Close
Full Screen / Esc	

Printer-friendly Version
Interactive Discussion

**Increasing transports
of volume, heat, and
salt towards the
Arctic in the Faroe
Current 1993–2013**

B. Hansen et al.

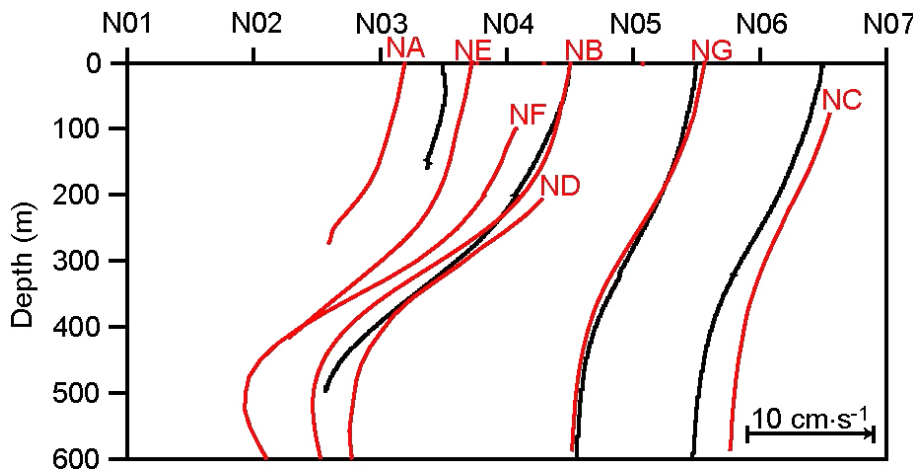


Figure 2. Average eastward geostrophic velocity profiles (black) between each pair of neighbouring standard stations from N03 to N07 and eastward ADCP velocity profiles from all sites (red). The surface expressions of the geostrophic profiles are located in the middle of the associated station pairs. For the long-term sites, the profiles have been extrapolated to the surface where they are located at the ADCP positions.

**Increasing transports
of volume, heat, and
salt towards the
Arctic in the Faroe
Current 1993–2013**

B. Hansen et al.

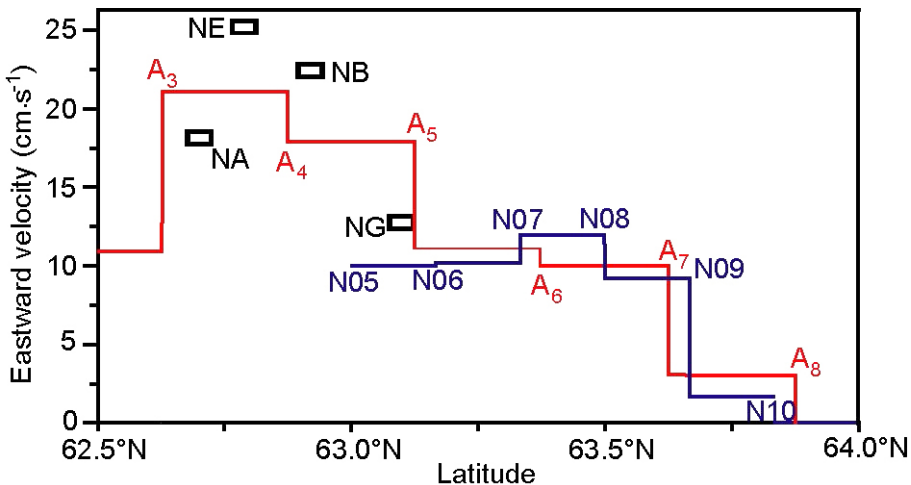


Figure 3. Values for the altimetry offset U_k^0 (red line) plotted together with average values for eastward surface velocity from the four long-term ADCP sites (rectangles) and from average geostrophy (Hansen et al., 2015, Table 2.4.3) (blue line).

Increasing transports of volume, heat, and salt towards the Arctic in the Faroe Current 1993–2013

B. Hansen et al.

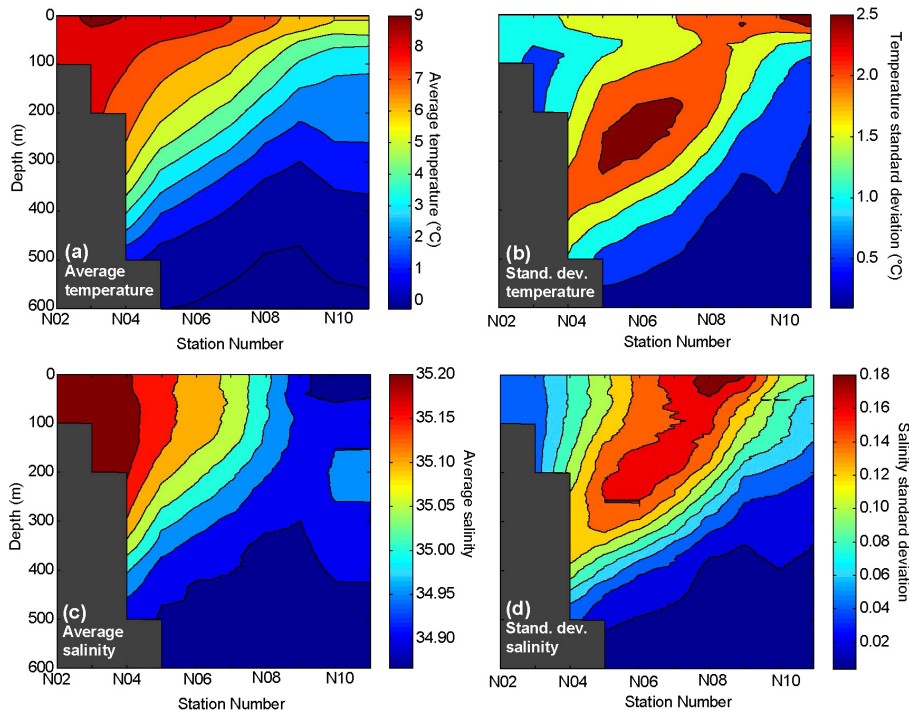


Figure 4. Hydrographic conditions on section N based on 78 CTD sections in the period 1993 to 2013. **(a)** Average temperature. **(b)** Standard deviation of temperature. **(c)** Average salinity. **(d)** Standard deviation of salinity. Grey areas indicate the bottom.

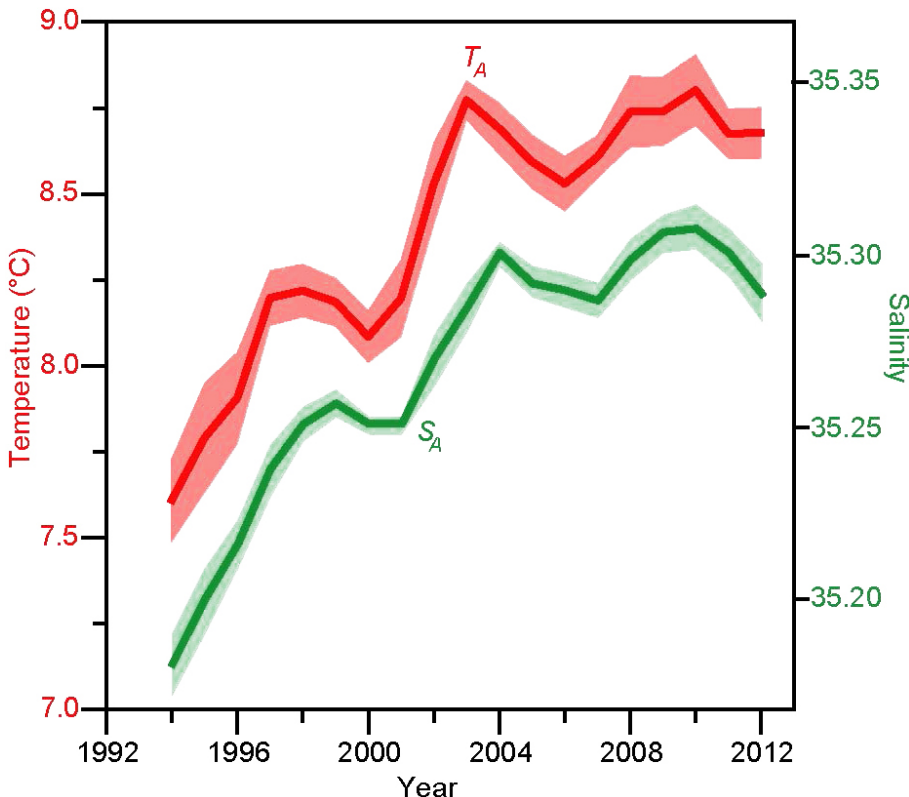


Figure 5. Long-term variation of Atlantic water temperature, T_A (red) and salinity, S_A (green). For each parameter, the figure shows 3 year running mean of deseasoned values (thick curves) with background colours indicating \pm one standard error over each 3 year period.

Increasing transports of volume, heat, and salt towards the Arctic in the Faroe Current 1993–2013

B. Hansen et al.

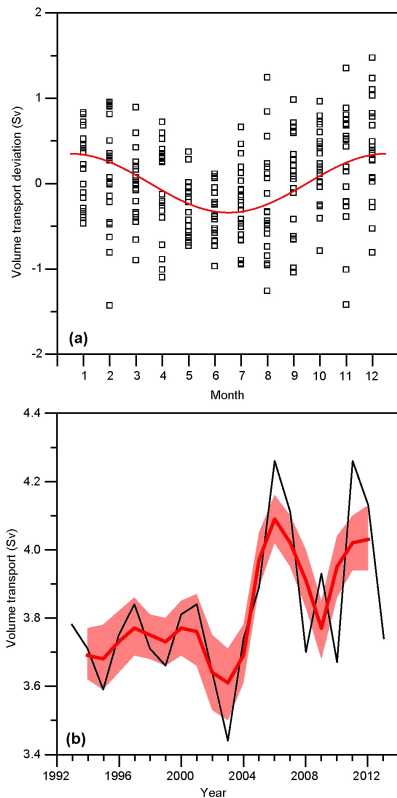


Figure 6. Seasonal **(a)** and long-term **(b)** variations of Atlantic water volume transport 1993–2013. **(a)** Each square represents transport deviation from the 3 year running mean for one month. The red curve represents the iteratively determined sinusoidal seasonal fit (Hansen et al., 2015, Appendix B). **(b)** Annually averaged transport (black curve) and 3 year averaged transport (red curve) with the red background representing \pm one standard error over each 3 year period.

**Increasing transports
of volume, heat, and
salt towards the
Arctic in the Faroe
Current 1993–2013**

B. Hansen et al.

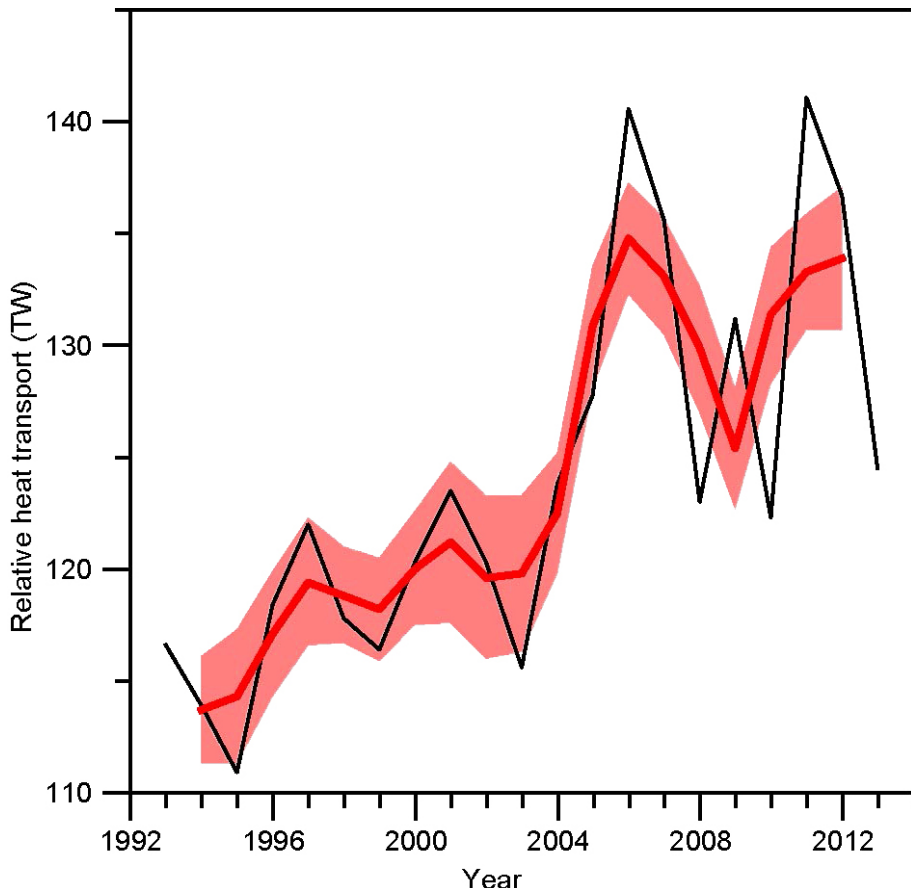


Figure 7. Long-term variation of relative (to 0 °C) heat transport 1993–2013. Annually averaged transport (black curve) and 3 year averaged transport (red curve) with the red background representing \pm one standard error over each 3 year period.

**Increasing transports
of volume, heat, and
salt towards the
Arctic in the Faroe
Current 1993–2013**

B. Hansen et al.

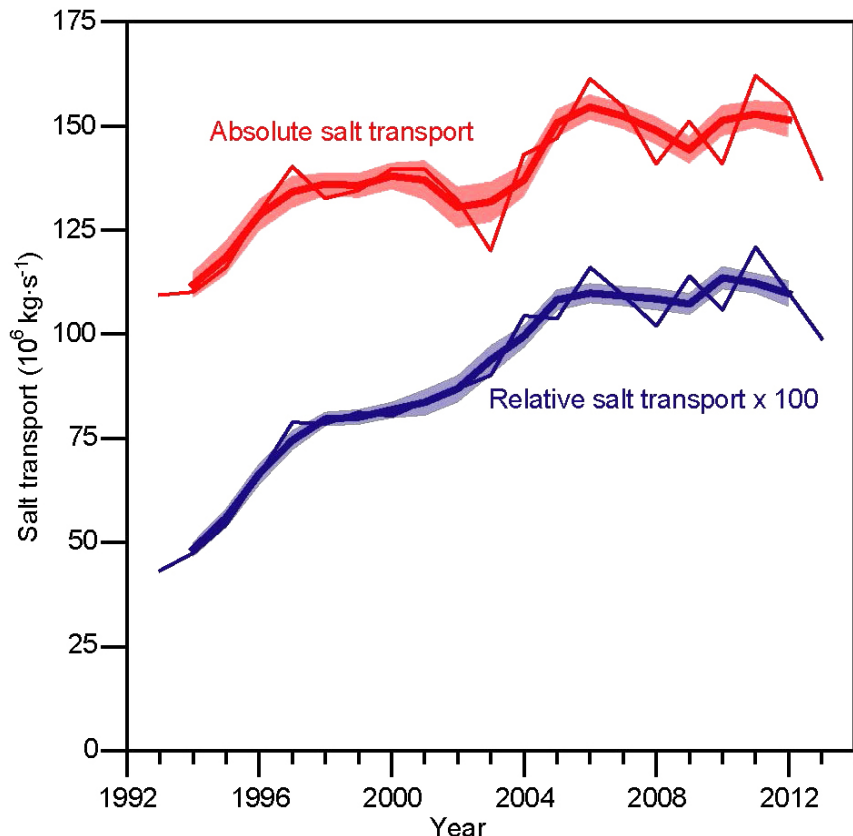


Figure 8. Long-term variation of absolute (red) and relative to 34.93 (blue) salt transport 1993–2013. Annually averaged transports (thin lines) and 3 year averaged transports (thick lines) with the background representing \pm one standard error over each 3 year period. The values for relative salt transport have been multiplied by 100 to fit the same scale as the absolute salt transport.